EXPLOITING FRI SIGNAL STRUCTURE FOR SUB-NYQUIST SAMPLING AND PROCESSING IN MEDICAL ULTRASOUND

Tanya Chernyakova and Yonina C. Eldar

Technion - Israel Institute of Technology
Dept. of Electrical Engineering
Haifa 32000, Israel

ABSTRACT

Signals consisting of short pulses are present in many applications including ultrawideband communication, object detection and navigation (radar, sonar) and medical imaging. The structure of such signals, effectively captured within the finite rate of innovation (FRI) framework, allows for significant reduction in sampling rates, required for perfect reconstruction. In this work we consider ultrasound imaging, where the FRI signal structure allows to reduce both sampling and processing rates. We show that beamforming, a crucial processing step in image generation that generally requires oversampling, can be implemented directly on reduced rate samples. This is obtained by replacing the standard time-domain processing by a frequency domain approach and relying on FRI sampling techniques in frequency. Using this approach we achieve significant rate reduction while retaining adequate image quality for both 2D and 3D imaging setups using data obtained by commercial imaging system.

***Index Terms*—** Array processing, finite rate of innovation, beamforming, ultrasound, sub-Nyquist sampling.

1. INTRODUCTION

When sampling an analog signal, we aim to represent it by discrete-time coefficients that capture its important features. The minimal sampling rate required for perfect reconstruction of bandlimited signals is defined by the classic Shannon-Nyquist as twice the maximal frequency. In many applications such rates are overwhelming. Luckily, the required sampling rate can be significantly reduced when additional information on signal structure is available. An interesting class of structured signals was suggested by Vetterli et al. [1], who considered signals with a finite number of degrees of freedom per unit time - signals with finite rate of innovation (FRI). One of the most studied cases of FRI signals is a stream of pulses, namely, a signal consisting of a stream of short pulses where the pulse shape is known. Such signals are presented in abundance in ultrawideband communication, object detection and navigation (radar, sonar) and medical imaging. In this work we consider an application of the FRI model to medical ultrasound imaging. Here FRI signal structure allows to reduce both sampling and processing rates far below the Nyquist rate of the signal.

Ultrasound imaging is performed by transmitting an acoustic pulse along a narrow beam from an array of transducer elements. During its propagation echoes are scattered by acoustic impedance perturbations in the tissue, and received by the array elements. The data, collected by the transducers, is sampled and digitally integrated in a way referred to as beamforming. The process of beamforming is comprised of averaging the received signals after their alignment with appropriate time-dependent delays. Beamforming allows to obtain a signal steered in a predefined direction, corresponding to the transmission path, and optimally focused at each depth. This results in signal-to-noise ratio (SNR) enhancement and improvement of angular localization. Such a beamformed signal, referred to as beam, forms a line in the image. Rates up to 4-10 times the central frequency of the transmitted pulse are typically required in order to eliminate artifacts caused by digital implementation of beamforming in time [2]. Taking into account the number of transducer elements and the number of lines in an image, the amount of sampled data that needs to be digitally processed is very large, motivating methods to reduce sampling and processing rates. The reduction in rate and, consequently, in amount of data can be particulary beneficial for portable devices and wireless probes.

Several frameworks reported in the literature [3, 4, 5] allow to sample and recover each individual received signal at a low-rate, while exploiting their structure and assuming sufficiently high SNR. However, the final goal in low-rate ultrasound imaging is to recover a 2D or 3D image. Such an image is obtained by integrating the noisy data sampled at multiple transducer channels. In standard imaging the integration is achieved by the process of beamforming, which is performed digitally and, theoretically, requires high sampling rates. Hence, in order to benefit from the rate reduction, achieved at the level of the received signals, one needs to be able to incorporate beamforming into the low-rate sampling process. Several works describe methods for recovering a beamformed signal from its low-rate samples using compressed sensing (CS) [6] methodology [7], [8], [9]. However, these techniques all assume that one has access to the continuous-time beamformed data. In practice, the beamformed signal is formed from samples of each of the individual received signals, so samples of the beamformed signal are not available at the transducer elements. Here we show that beamforming can be implemented directly on reduced rate samples by replacing the standard time-domain processing by a frequency domain approach [10, 11] and relying on previous FRI sampling techniques in frequency [3, 12, 10]. The proposed method is demonstrated on data obtained by commercial imaging system for both 2D and 3D imaging modes. The resulting images retain adequate image quality, while the rates are reduced far below Nyquist.

The rest of the paper is organized as follows: in Section 2, we review beamforming in time. The FRI model of beamformed signal is introduced in Section 3. In Section 4 we show that beamforming can be performed directly in frequency using low-rate samples of individual elements and introduce low-rate sampling approach. The performance of the proposed method for both 2D and 3D imaging modes is demonstrated in Section 5. Section 6 concludes the paper.

2. CONVENTIONAL PROCESSING

To derive an equation corresponding to the process of beamforming we consider an array comprised of M transceiver elements, as illustrated in Fig. 1. The reference element m_0 is set at the origin. Denote by δ_m its distance to the mth element and by c the speed of sound. A pulse of acoustic energy, transmitted at the direction θ,

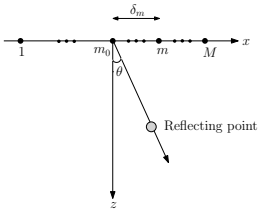

Fig. 1. M receivers aligned along the x axis. An acoustic pulse is transmitted in a direction θ. The echoes scattered from perturbation in the radiated tissue are received by the array elements.

reaches coordinates $(x, z) = (ct\sin\theta, ct\cos\theta)$ at time $t \geq 0$. An echo originating from a scatterer located at this position will be received by all array elements at a time depending on their locations. Denote by $\varphi_m(t)$ the signal received by the mth element and by $\hat{\tau}_m(t;\theta)$ the time of arrival. It is readily seen that:

$$\hat{\tau}_m(t;\theta) = t + \frac{d_m(t;\theta)}{c}, \tag{1}$$

where $d_m(t;\theta) = \sqrt{(ct\cos\theta)^2 + (\delta_m - ct\sin\theta)^2}$ is the distance traveled by the reflection.

Using (1), the arrival time at m_0 is $\hat{\tau}_{m_0}(t;\theta) = 2t$. Applying an appropriate delay to $\varphi_m(t)$, such that the resulting signal $\hat{\varphi}_m(t;\theta)$ satisfies $\hat{\varphi}_m(2t;\theta) = \varphi_m(\hat{\tau}_m(t;\theta))$, we can align the reflection received by the mth receiver with the one received at m_0. Denoting $\tau_m(t;\theta) = \hat{\tau}_m(t/2;\theta)$ and using (1), the following aligned signal is obtained:

$$\begin{aligned}\hat{\varphi}_m(t;\theta) &= \varphi_m(\tau_m(t;\theta)), \\ \tau_m(t;\theta) &= \frac{1}{2}\left(t + \sqrt{t^2 - 4(\delta_m/c)t\sin\theta + 4(\delta_m/c)^2}\right).\end{aligned} \tag{2}$$

The beamformed signal may now be derived by averaging the aligned signals:

$$\Phi(t;\theta) = \frac{1}{M}\sum_{m=1}^{M}\hat{\varphi}_m(t;\theta). \tag{3}$$

Such a beam is optimally focused at each depth and hence exhibits improved angular localization and enhanced SNR.

Although defined over continuous time, modern imaging systems perform the beamforming in (2)-(3) in the digital domain. This allows to apply dynamically changing delays of (2) on sampled and stored channel data. Digital implementation of beamforming, however, requires severe oversampling of the received signals since the Nyquist rate is insufficient due to the high delay resolution needed. The required sampling rates are usually 4-10 times the transducer central frequency [2]. In the sequel we denote the rate required to avoid artifacts in digital implementation of beamforming, as the beamforming rate f_s.

In this paper we show that by translation of the beamforming process to the frequency domain and by exploiting the FRI structure of the beam we are able not only to avoid oversampling, but both sample and process the data at sub-Nyquist rates.

3. FRI MODEL OF ULTRASOUND SIGNAL

According to [10], a beamformed signal obeys an FRI model, namely, it can be modeled as a sum of replicas of the known transmitted pulse, $h(t)$, with unknown amplitudes and delays:

$$\Phi(t;\theta) \simeq \sum_{l=1}^{L} b_l h(t - t_l). \tag{4}$$

Here L is the number of scattering elements in direction θ, $\{b_l\}_{l=1}^{L}$ are the unknown amplitudes of the reflections and $\{t_l\}_{l=1}^{L}$ denote the times at which the reflection from the lth element arrived at the receiver m_0. The Fourier coefficients of the beam are given by:

$$c[k] = h[k]\sum_{l=1}^{L} b_l e^{-i\frac{2\pi}{T}kt_l}, \tag{5}$$

where $h[k]$ is the Fourier coefficient of the transmitted pulse. By quantizing the delays $\{t_l\}_{l=1}^{L}$ with quantization step $T_s = \frac{1}{f_s}$, such that $t_l = q_l T_s, q_l \in \mathbb{Z}$, we may write the Fourier coefficients of the beamformed signal as:

$$c[k] = h[k]\sum_{l=1}^{L} b_l e^{-i\frac{2\pi}{T}kq_l T_s}. \tag{6}$$

Assume we have a subset μ_{BF}, $|\mu_{BF}| = M_{BF}$, of beam's Fourier coefficients. Denoting by N the ratio $\lfloor T/T_s \rfloor$ we can recast (6) in vector-matrix notation:

$$\mathbf{c} = \mathbf{HDb} = \mathbf{Ab}, \tag{7}$$

where $\mathbf{H}$ is an $M_{BF} \times M_{BF}$ diagonal matrix with $h[k]$ as its kth entry, $\mathbf{D}$ is an $M_{BF} \times N$ matrix formed by taking the set μ_{BF} of rows from an $N \times N$ Fourier matrix, and $\mathbf{b}$ is a length-N vector whose kth entry equals b_l for $k = q_l$ and 0 otherwise.

Our goal is to determine $\mathbf{b}$ from a length-M_{BF} measurement vector $\mathbf{c}$. To this end we note that a beamformed ultrasound signal is typically comprised of a relatively small number of strong reflections and many scattered echoes, that are on average at least two orders of magnitude weaker. It is, therefore, natural to assume that the coefficient vector $\mathbf{b}$, defined in (7), is compressible or approximately sparse. This property of $\mathbf{b}$ can be captured by using the l_1 norm, leading to the optimization problem:

$$\min_{\mathbf{b}} \|\mathbf{b}\|_1 \quad \text{subject to} \quad \|\mathbf{Ab} - \mathbf{c}\|_2 \leq \varepsilon. \tag{8}$$

Problem (8) is a classic CS problem and can be solved using second-order methods such as interior point methods [13], [14] or first-order methods, based on iterative shrinkage ideas [15], [16].

4. FREQUENCY DOMAIN BEAMFORMING AND LOW-RATE SAMPLING

We have shown that a beamformed signal can be recovered from a small subset of μ_{BF} of its Fourier coefficients. However, sampling is performed in time prior to beamforming. The question is how can we obtain frequency samples of the beam from low-rate time samples of the received signals?

4.1. Beamforming in Frequency

To this end we use the fact that beamforming can be performed equivalently directly in frequency, namely, Fourier coefficients of the beam can be obtained as a linear combination of Fourier coefficients of the received signals [10, 11].

Denote the Fourier series coefficients of $\Phi(t;\theta)$ with respect to the interval $[0,T)$ by

$$c[k] = \frac{1}{T}\int_0^T I_{[0,T_B(\theta))}(t)\Phi(t;\theta)e^{-i\frac{2\pi}{T}kt}dt, \tag{9}$$

where $I_{[a,b)}$ is the indicator function equal to 1 when $a \le t < b$ and 0 otherwise, T is defined by the transmitted pulse penetration depth and $T_B(\theta) = \min_{1\le m\le M}\tau_m^{-1}(T;\theta) < T$ defines the support of the beam as shown in [10]. Plugging (2) and (3) into (9), we get:

$$c[k] = \frac{1}{M}\sum_{m=1}^{M}\frac{1}{T}\int_0^T I_{[0,T_B(\theta))}(t)\varphi_m(\tau_m(t;\theta))e^{-i\frac{2\pi}{T}kt}dt. \tag{10}$$

After some algebraic manipulation we obtain:

$$c[k] = \frac{1}{M}\sum_{m=1}^{M}\frac{1}{T}\int_0^T \varphi_m(t)q_{k,m}(t;\theta)e^{-i\frac{2\pi}{T}kt}dt, \tag{11}$$

with

$$q_{k,m}(t;\theta) = I_{[|\gamma_m|,\tau_m(T;\theta))}(t)\left(1+\frac{\gamma_m^2\cos^2\theta}{(t-\gamma_m\sin\theta)^2}\right)\times \exp\left\{i\frac{2\pi}{T}k\frac{\gamma_m - t\sin\theta}{t-\gamma_m\sin\theta}\gamma_m\right\}, \tag{12}$$

and $\gamma_m = \delta_m/c$. Note that (11) contains a non-delayed version of $\varphi_m(t)$, in contrast to (10). The delays are effectively applied through the distortion function, $q_{k,m}(t;\theta)$, defined in (12).

We next replace $\varphi_m(t)$ by its Fourier series coefficients. Denoting the nth Fourier coefficient by $c_m[n]$ we can rewrite (11) as

$$\begin{aligned} c[k] &= \frac{1}{M}\sum_{m=1}^{M}\sum_n c_m[n]\frac{1}{T}\int_0^T q_{k,m}(t;\theta)e^{-i\frac{2\pi}{T}(k-n)t}dt \\ &= \frac{1}{M}\sum_{m=1}^{M}\sum_n c_m[k-n]Q_{k,m;\theta}[n], \end{aligned} \tag{13}$$

where $Q_{k,m;\theta}[n]$ are the Fourier coefficients of $q_{k,m}(t;\theta)$ with respect to $[0,T)$. When substituted by its Fourier coefficients, the distortion function effectively transfers the beamforming delays defined in (2) to the frequency domain. The function $q_{k,m}(t;\theta)$ depends only on the array geometry and is independent of the received signals. Therefore, its Fourier coefficients can be computed off-line and used as a look-up-table (LUT) during the imaging cycle.

In addition, as shown in [11], most of the energy of the set $\{Q_{k,m;\theta}[n]\}$ is concentrated around the direct current (DC) component and its decaying properties allow to rewrite (13) as

$$c[k] \simeq \frac{1}{M}\sum_{m=1}^{M}\sum_{n=-N_1}^{N_2} c_m[k-n]Q_{k,m;\theta}[n], \tag{14}$$

where the choice of N_1 and N_2 controls the approximation quality.

Derivations of frequency domain beamforming can be extended to 3D imaging mode [17]. To this end we need to take into account the 2D geometry of the transducer and an additional steering angle, required to span the 3D volume of interest. As shown in [17], these changes affect the distortion function defined in (12), however, the decaying property of its Fourier coefficients remains unchanged and (13) remains valid.

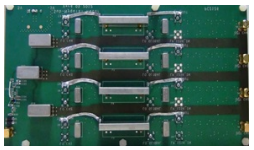

Fig. 2. A Xampling-based hardware prototype for sub-Nyquist sampling. The prototype computes low-rate samples of the input from which the required set of Fourier coefficients can be computed.

4.2. Low Rate Sampling

Denote by β the set of Fourier coefficients of the received signal that correspond to its bandwidth, namely, the values of k for which $c_m[k]$ is nonzero (or larger than a threshold). Let B denote the cardinality of β. Note that (14) implies, that the bandwidth of the beamformed signal, β_{BF}, will contain at most $(B+N_1+N_2)$ nonzero frequency components. In a typical imaging setup the size of B is on the order of hundreds, while N_1 and N_2, defined by the decay properties of $\{Q_{k,m;\theta}[n]\}$, are typically no larger than 10. This implies that $B + N_1 + N_2 \approx B$, so that the bandwidth of the beam is approximately equal to the bandwidth of the received signals.

To compute the elements in β_{BF} according to (14) we need a set β of each of the received signals. This allows to exploit the low effective bandwidth of the received signals and apply beamforming at a rate corresponding to the effective Nyquist rate of the received signals, namely, the signal's effective bandpass bandwidth. In this way we avoid oversampling required by digital implementation of beamforming in time, assuming that it is possible to obtain the required set β for each one of the received signals by sampling at the effective Nyquist rate.

A general approach to this problem is to use the Xampling mechanism proposed in [3]. Xampling allows to obtain an arbitrary set κ, comprised of K frequency components, from K point-wise samples of the signal filtered with an appropriate analog kernel $s^*(-t)$. The kernel is designed according to the required set κ. It effectively zeros those frequency components of the signal that are not included in κ. The required Fourier coefficients are equal to the Fourier transform of the output, therefore, the number of taken samples is equal to the number of Fourier coefficients of interest. Theoretically, for a general and possibly non-consecutive set of frequency components the Sum of Sincs kernel can be used [3]. Practical aspects of the Xampling approach implementation for sub-Nyquist sampling of radar signals are considered in [18]. This work led to the implementation of a hardware Xampling prototype, shown in Fig. 2, allowing to sample radar signals far below their Nyquist rate.

In the context of ultrasound imaging a simpler sampling approach is often possible. We aim to obtain a consecutive set β of the Fourier coefficients of the received signals. This can be achieved by filtering the received signal with a simple band-pass filter, corresponding to the frequency band, defined by β. The resulting signal can then be sampled at the Nyquist rate, defined with respect to the bandwidth of β, using band-pass [19] or quadrature sampling [20] techniques. Applying the Fourier transform to the resulting low-rate samples yields the required set β. In this approach the received signals are sampled at their effective Nyquist rate.

Further reduction in rate can be achieved if we want to obtain only a partial frequency beam's data as discussed in Section 3. Explicitly, assume that now we are interested in $\mu_{BF} \subset \beta_{BF}$ of size M_{BF} of Fourier coefficients of the beam. We note that according to (14) μ_{BF} can be calculated from at most $M = (M_{BF} + N_1 + N_2)$ Fourier coefficients of each one of the received signals. Denote the

required subset of M coefficients of the received signal by μ. In this case the received signals are sampled at a rate which is N/M lower than the standard beamforming rate and B/M lower than their effective Nyquist rate, while the required analog kernel is defined by the subset μ_{BF}.

The choice of μ_{BF} and consequently the analog kernel is dictated by the transmitted pulse shape. When imaging is performed with a modulated Gaussian pulse, the optimal choice of μ_{BF} is to take M consecutive elements around the cental frequency. This choice captures the maximal amount of signal energy and can be implemented with a band-pass filter defined by the frequency band corresponding to μ_{BF}.

On the other hand, if the spectrum of the transmitted pulse is flat, which is the case for linear frequency-modulated chirps [21], [22], then the performance of CS recovery improves when μ_{BF} is comprised of elements of β chosen uniformly at random. The resulting sampling operation can be implemented using the techniques proposed in [3] and [18].

The entire scheme, performing low-rate sampling and frequency domain beamforming, is depicted in Fig. 3. Signals $\{\varphi_m(t)\}_{m=1}^{M}$, received at each transducer element, are filtered with an appropriate analog kernel $s^*(-t)$ and sampled at a low-rate. Both the analog kernel and the sampling rate are defined by the set of Fourier coefficients of interest. Fourier coefficients of the received signals are then computed and beamforming is performed directly in frequency at a low-rate using (14).

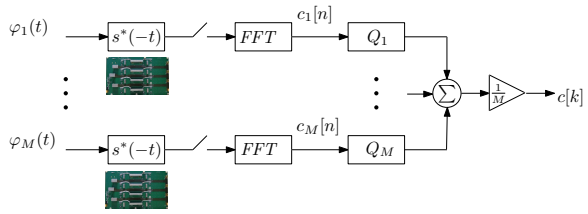

Fig. 3. Fourier domain beamforming scheme. The block Q_i represents averaging the Fourier coefficients according to (14).

5. RESULTS

To demonstrate low-rate beamforming in frequency we simulated digitally the application of our technique on in vivo cardiac data. Data acquisition is performed with $f_s = 16$ MHz, leading to $N = 3360$ samples for 16 cm imaging depth. To perform beamforming in frequency we used a subset μ_{BF} of 100 Fourier coefficients, which can be obtained from $M = 120$ low-rate samples by the scheme illustrated in Fig. 3 with an appropriate choice of band-pass filter. This implies 28 fold reduction in sampling and 14 fold reduction in processing rate compared to standard beamforming, which requires 3360 samples for this particular imaging setup. The difference between the sampling and processing rates stems from the complex nature of Fourier coefficients. Having computed the Fourier coefficients of the beamformed signal, we obtain its parametric representation by solving (8). To this end we used the NESTA algorithm [23]. The resulting images, corresponding to two different frames, are shown in Fig. 4.

We next demonstrate our method on data collected using a commercial 3D imaging system. We process the data collected in the imaging of a phantom of a heart ventricle. In this setup frequency domain beamforming together with exploiting FRI structure of the resulting signals allow to obtain 11-fold rate reduction while retaining adequate image quality as can be seen in Fig. 5. In this case frequency domain beamforming is performed using 273 Fourier coefficients, while time domain processing requires 3120 samples.

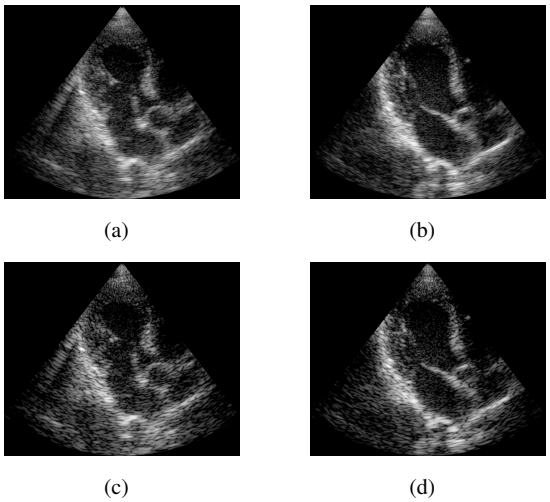

(a) (b) (c) (d)

Fig. 4. Cardiac images constructed with different beamforming techniques. The first column, (a), (c), corresponds to frame 1, the second column, (b), (d), corresponds to frame 2. (a), (b) Time domain beamforming. (c), (d) Low-rate frequency domain beamforming.

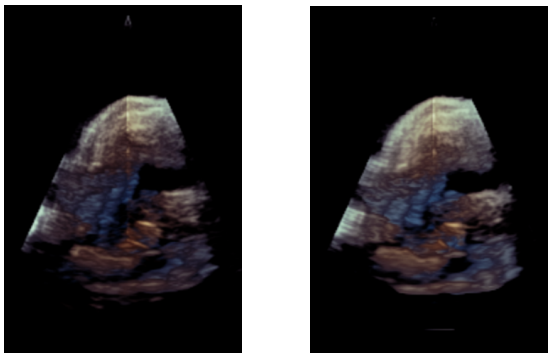

(a) (b)

Fig. 5. 3D imaging of a heart ventricle phantom .(a) Time domain beamforming. (b) Low-rate frequency domain beamforming.

6. CONCLUSIONS

In this work we propose a framework enabling low-rate ultrasound imaging, including the step of sub-Nyquist data acquisition, low-rate processing and beamformed signal reconstruction. The proposed framework is based on Xampling and frequency domain beamforming and exploits FRI structure of ultrasound signals. It allows not only to sample the received signals at a low-rate, but also enables low-rate processing, closing the gap between the acquisition of the raw data and reconstruction of the beamformed signals, comprising the resulting image. Our results prove that the concept of sub-Nyquist processing is feasible for medical ultrasound, leading to the potential of considerable reduction in future ultrasound machines size, power consumption and cost.

7. REFERENCES

[1] M. Vetterli, P. Marziliano, and T. Blu, "Sampling signals with finite rate of innovation," *IEEE Transactions on Signal Processing*, vol. 50, no. 6, pp. 1417–1428, 2002.

[2] B. D. Steinberg, "Digital beamforming in ultrasound," *IEEE Transactions on Ultrasonics, Ferroelectrics and Frequency Control*, vol. 39, no. 6, pp. 716–721, 1992.

[3] R. Tur, Y. C. Eldar, and Z. Friedman, "Innovation rate sampling of pulse streams with application to ultrasound imaging," *IEEE Transactions on Signal Processing*, vol. 59, no. 4, pp. 1827–1842, 2011.

[4] X. Zhuang, Y. Zhao, Z. Dai, H. Wang, and L. Wang, "Ultrasonic signal compressive detection with sub-nyquist sampling rate," *Journal of Scientific and Industrial Research*, vol. 71, pp. 195–199, 2012.

[5] H. Liebgott, R. Prost, and D. Friboulet, "Pre-beamformed rf signal reconstruction in medical ultrasound using compressive sensing," *Ultrasonics*, 2012.

[6] Y. C. Eldar and G. Kutyniok, *Compressed sensing: theory and applications*, Cambridge University Press, 2012.

[7] A. Achim, B. Buxton, G. Tzagkarakis, and P. Tsakalides, "Compressive sensing for ultrasound rf echoes using a-stable distributions," in *Engineering in Medicine and Biology Society (EMBC), 2010 Annual International Conference of the IEEE*. IEEE, 2010, pp. 4304–4307.

[8] G. Tzagkarakis, A. Achim, P. Tsakalides, and J-L Starck, "Joint reconstruction of compressively sensed ultrasound rf echoes by exploiting temporal correlations," in *2013 IEEE 10th International Symposium on Biomedical Imaging (ISBI)*. IEEE, 2013, pp. 632–635.

[9] C. Quinsac, A. Basarab, and D. Kouamé, "Frequency domain compressive sampling for ultrasound imaging," *Advances in Acoustics and Vibration*, vol. 2012, 2012.

[10] N. Wagner, Y. C. Eldar, and Z. Friedman, "Compressed beamforming in ultrasound imaging," *IEEE Transactions on Signal Processing*, vol. 60, no. 9, pp. 4643–4657, 2012.

[11] T. Chernyakova and Y. C. Eldar, "Fourier domain beamforming: The path to compressed ultrasound imaging," *IEEE Transactions on Ultrasonics, Ferroelectronics, and Frequency Control*, vol. 61, no. 8, pp. 1252–1267, 2014.

[12] K. Gedalyahu, R. Tur, and Y. C. Eldar, "Multichannel sampling of pulse streams at the rate of innovation," *IEEE Transactions on Signal Processing*, vol. 59, no. 4, pp. 1491–1504, 2011.

[13] E. Candès and J. Romberg, "l1-magic," *www. l1-magic. org*, 2007.

[14] M. Grant, S. Boyd, and Y. Ye, "CVX: Matlab software for disciplined convex programming," 2008.

[15] A. Beck and M. Teboulle, "A fast iterative shrinkage-thresholding algorithm for linear inverse problems," *SIAM Journal on Imaging Sciences*, vol. 2, no. 1, pp. 183–202, 2009.

[16] E. T. Hale, W. Yin, and Y. Zhang, "A fixed-point continuation method for l1-regularized minimization with applications to compressed sensing," *CAAM TR07-07, Rice University*, 2007.

[17] M. Birk, A. Burshtein, T. Chernyakova, A. Eilam, J. W. Choe, A. Nikoozadeh, P. Khuri-Yakub, and Y. C. Eldar, "Compressed 3D ultrasound imaging with 2D arrays," ICASSP 2014.

[18] E. Baransky, G. Itzhak, I. Shmuel, N. Wagner, E. Shoshan, and Y. C. Eldar, "A sub-nyquist radar prototype: Hardware and algorithms," *IEEE Transactions on Aerospace and Electronic Systems, special issue on Compressed Sensing for Radar*, vol. 50, no. 2, pp. 809–822, 2014.

[19] R. G. Vaughan, N. L. Scott, and D. R. White, "The theory of bandpass sampling," *IEEE Transactions on Signal Processing*, vol. 39, no. 9, pp. 1973–1984, 1991.

[20] O. D. Grace and S. P. Pitt, "Sampling and interpolation of bandlimited signals by quadrature methods," *The Journal of the Acoustical Society of America*, vol. 48, pp. 1311, 1970.

[21] T. Misaridis and J. A. Jensen, "Use of modulated excitation signals in medical ultrasound. Part I: Basic concepts and expected benefits," *IEEE Transactions on Ultrasonics, Ferroelectrics and Frequency Control*, vol. 52, no. 2, pp. 177–191, 2005.

[22] J. M. G. Borsboom, C. T. Chin, A. Bouakaz, M. Versluis, and N. de Jong, "Harmonic chirp imaging method for ultrasound contrast agent," *IEEE Transactions on Ultrasonics, Ferroelectrics and Frequency Control*, vol. 52, no. 2, pp. 241–249, 2005.

[23] S. Becker, J. Bobin, and E. J. Candès, "NESTA: a fast and accurate first-order method for sparse recovery," *SIAM Journal on Imaging Sciences*, vol. 4, no. 1, pp. 1–39, 2011.